



Cite this: *Green Chem.*, 2024, **26**, 6124

## Hydride-free reduction of propargyl electrophiles: a nickel-catalyzed photoredox strategy for allene synthesis†

Tingjun Hu,<sup>a</sup> Vincent Fagué,<sup>a</sup> Didier Bouyssi,<sup>a</sup> Nuno Monteiro<sup>a</sup> and Abderrahmane Amgoune  <sup>\*a,b</sup>

Herein we report a catalytic reduction of propargyl carbonates to allenes mediated by a nickel molecular catalyst. The catalytic system uses light as the driving force and amine as the sole hydrogen source. Contrary to other catalytic approaches, the process proceeds without the intermediacy of metal hydride species. The commonly observed pathway in transition metal catalyzed reductive processes is replaced by a pathway involving a sequence of electron transfer and proton transfer. Using this catalytic approach, a wide range of allenes could be obtained under mild conditions. Experimental investigations support the dual role of trialkylamine as a reductant and a proton source and have revealed the key mechanistic features of the reaction. A key protodemetallation step of the Ni(II) allenyl intermediate is proposed to account for the reduction process. Finally, we also demonstrate that the selective S<sub>N</sub><sup>2'</sup> reduction process can be also efficiently driven by an electrochemical approach.

Received 27th February 2024,  
Accepted 1st April 2024

DOI: 10.1039/d4gc00984c

rsc.li/greenchem

## Introduction

Allenes are key intermediates in organic synthesis, offering a rich palette of chemical reactivity and serving as essential building blocks in the construction of complex molecules. They are important structural motifs found in natural products and pharmaceuticals, and used to design advanced functional materials as well, making them interesting target molecules.<sup>1</sup> In this regard, transition metal-catalyzed reactions of propargyl electrophiles with nucleophilic partners stand among the most attractive strategies for constructing allene motifs featuring otherwise difficult-to-access substitution patterns and functionalities. A long-standing challenge in the development of such methods has been the difficulty in predicting and controlling regioselectivity (S<sub>N</sub><sup>2</sup> vs. S<sub>N</sub><sup>2'</sup> selectivity), and thus preventing the formation of isomeric propargylic by-products.<sup>2</sup>

In this domain, catalytic hydride reductions of propargyl halides and propargyl alcohol derivatives have emerged as established methodologies since the mid-80s, serving as practical tools for the synthesis of mono- to tri-substituted allenes. Traditional methods rely essentially on palladium<sup>3</sup> or copper<sup>4</sup>

catalysis in combination with conventional hydride-based reducing agents, *i.e.* aluminium or boron hydrides,<sup>3b,4e</sup> formates,<sup>3c,4b</sup> and silanes.<sup>4a,c,d</sup> In these processes, transition metal hydrides serve as key intermediates (Fig. 1A). However, the reliance on stoichiometric Al, B, and Si-based metalloids often in conjunction with a noble transition metal can limit broader applications with respect to functional group tolerance, safety, and sustainability concerns.

Complementary to conventional thermal protocols, photo- or electrocatalytic processes provide practical and efficient routes for catalytic reduction reactions, harnessing electrons and protons as redox equivalents, and thus obviating the use of hydrogen gas or hydride donors.<sup>5</sup> From a mechanistic standpoint, all these methodologies rely on the formation of metal hydrides as catalytically relevant intermediates. More recently, alternative pathways exempt of hydride intermediates have attracted increasing interest as sustainable and cost-effective strategies for hydrogenation/reduction processes.<sup>5a,b</sup> The reaction manifolds involve a reduction of the transition metal catalyst that activates the substrate followed by protonation. In this context, we present a novel nickel-catalyzed photoredox reduction strategy for a selective, sustainable and robust access to diversely substituted allenes under mild reaction conditions from propargyl electrophiles.<sup>6</sup> Unlike traditional methods, our approach eliminates the requirement for hydride nucleophiles, instead relying on protodemetallation of an allenylmetal intermediate. Notably, we demonstrate that a trialkylamine plays the roles of both a redox mediator, as a reductive

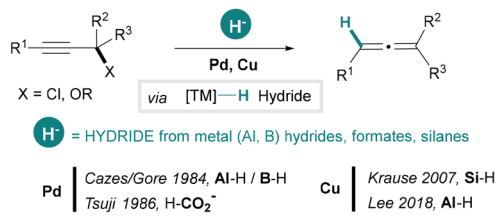
<sup>a</sup>Université Lyon 1, Institut de Chimie et Biochimie Moléculaires et Supramoléculaires, UMR 5246 du CNRS, 1, rue Victor Grignard, 69100 Villeurbanne, France. E-mail: [abderrahmane.amgoune@univ-lyon1.fr](mailto:abderrahmane.amgoune@univ-lyon1.fr)

<sup>b</sup>Institut Universitaire de France (IUF), 1 rue Descartes, 75231 Paris, France

† Electronic supplementary information (ESI) available. See DOI: <https://doi.org/10.1039/d4gc00984c>



## A. Traditional methods: Pd(or Cu)-catalyzed hydride reductions.



## B. This work: Ni/photoredox-catalyzed hydride-free reduction.

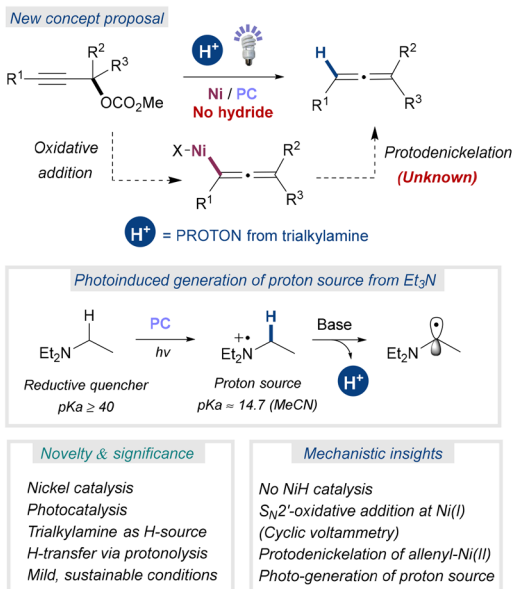


**Fig. 1** Synthetic methods for allenes involving transition metal (TM)-catalyzed reduction of propargyl electrophiles.

quencher of the photocatalytic cycle, and a proton source, *via* proton transfer from its photochemically generated amine radical cation (Fig. 1B).<sup>7,8</sup>

## Results and discussion

### Development and optimization studies

Preliminary studies have focused on the reduction of alk-2-ynyl carbonate **1a** as a model substrate (Table 1). Extensive experimentation led to the identification of nickel(II) nitrate, 1,10-phenanthroline (**2**), and 9,10-diphenylanthracene (DPA, **3a**) as an effective and inexpensive nickel source, ligand and organophotocatalyst, respectively. DPA is commonly used as an organic semi-conductor in OLEDs and in blue glow sticks; however, its potential as an effective photocatalyst has only been illustrated very recently.<sup>9</sup> Acetone, a sustainable and non-toxic solvent, was also identified as an appropriate medium for the reaction. Thus, when the reduction of **1a** was performed in the presence of triethylamine (1 equiv.) with 5 mol% of catalyst and ligand each under purple light (405 nm) irradiation, the corresponding allene **6** was produced exclusively within 3 h, and in almost quantitative spectroscopic yield (96%, <sup>19</sup>F NMR)

**Table 1** Selected preliminary optimization experiments<sup>a</sup>

$$\text{1a} \xrightarrow[\text{405 nm}]{\text{5 mol\% DPA, 5 mol\% Ni(NO}_3)_2 \cdot 6\text{H}_2\text{O, 5 mol\% 1,10-Phen, Et}_3\text{N (1 equiv.), Acetone (0.1 M), rt, 3 h}} \text{6}$$

R = CO<sub>2</sub>Me

Entry	Deviation from the above reaction	Yield <sup>b</sup>
1	None	96
2	Ni(COD) <sub>2</sub> /1,10-Phen as catalyst	56
3	No nickel salt	0
4	No ligand	0
5	No photocatalyst (light only)	0
6	No light (dark)	0
7	w/o Et <sub>3</sub> N	0
8	Quinclidine instead of Et <sub>3</sub> N	0
9	[Ir(dF(CF <sub>3</sub> )ppy) <sub>2</sub> (dtbbpy)]PF <sub>6</sub> (1 mol%) as PC	66
10	4-CzIPN (2 mol%) as PC	53
11	1 mol% DPA (24 h)	78
12	1 mol% DPA-OMe (24 h)	99
13	1 mol% DPA-CO <sub>2</sub> Me (24 h)	99
14	1 mol% DPA-CO <sub>2</sub> H (48 h) <sup>c</sup>	80
15	1 mol% DPA-OMe, 2 mol% [Ni/L] (24 h)	81
16	1 mol% DPA-CO <sub>2</sub> Me, 2 mol% [Ni/L] (24 h)	89
17	R = Boc	78
18	R = Ac	36 <sup>d</sup>

**DPA** (R = H, **3a**)  
**DPA-OMe** (R = OMe, **3b**)  
**DPA-CO<sub>2</sub>Me** (R = CO<sub>2</sub>Me, **3c**)  
**DPA-CO<sub>2</sub>H** (R = CO<sub>2</sub>H, **3d**)

**4-CzIPN** (**4**)

**Ir[dF(CF<sub>3</sub>)ppy]<sub>2</sub>(dtbbpy)PF<sub>6</sub>** (**5**)

<sup>a</sup> Reactions were performed on a 0.25 mmol scale using an EvluChem™ PhotoRedOx Box device equipped with one 18 W purple LED lamp (405 nm). Dtbppy = 4,4'-di-*tert*-butyl-2,2'-dipyridyl. <sup>b</sup> Yields (%) were determined by <sup>19</sup>F NMR spectroscopy using fluorobenzene as an internal standard. <sup>c</sup> 1.1 equiv. of Et<sub>3</sub>N were used. Approximately 20% of **1a** remained unreacted. <sup>d</sup> 38% conversion.

(Table 1, entry 1). The reaction also proceeded but to a lesser extent with the air-sensitive Ni(COD)<sub>2</sub>/1,10-Phen catalytic system (Table 1, entry 2). Control experiments confirmed that the dual catalytic system, light irradiation, and triethylamine are essential for this transformation (Table 1, entries 3–7). 1,2,3,5-Tetrakis(carbazol-9-yl)-4,6-dicyano-benzene (4-CzIPN, **4**) as well as the iridium complex Ir[dF(CF<sub>3</sub>)ppy]<sub>2</sub>(dtbbpy)PF<sub>6</sub> (**5**) proved to be competent alternative photocatalysts. However, the reaction efficiency is compromised by concomitant formation of several unidentified by-products, most likely generated from photo-degradation of the desired allenic product, leading to lower yields (Table 1, entries 9 and 10; and Table S6, ESI†). Furthermore, the reaction proceeded well with lower loadings of DPA, down to 1 mol%, provided that the reaction time was extended to 24 h (Table 1, entry 11). Other DPA derivatives were also investigated. Remarkably, both 9-(4-methoxyphenyl)-10-phenyl-anthracene (DPA-OMe, **3b**) and 9-(4-methoxycarbonylphenyl)-10-phenylanthracene (DPA-CO<sub>2</sub>Me, **3c**) had a beneficial effect on the reaction, affording quantitat-



ive yields of **6** (Table 1, entries 12 and 13). Interestingly, a carboxylic acid derivative (DPA-CO<sub>2</sub>H, **3d**) also showed significant photocatalytic activity, although the reaction was hampered by slower reaction rates (Table 1, entry 14).<sup>10</sup> Under the improved reaction conditions, a nickel catalyst loading of 2 mol% was still sufficient for excellent catalytic activity within 24 h, especially with DPA-CO<sub>2</sub>Me as the photocatalyst (Table 1, entries 15 and 16). Finally, we identified the OBoc group as a competent alternative leaving group, where OAc proved less efficient (Table 1, entries 17 and 18).

### Scope and limitations

The substrate scope was subsequently explored under our standard set of reaction conditions using a broad range of propargylic carbonates featuring diverse substitution patterns. Structurally diverse mono- to tri-substituted allenes could be delivered regioselectively in good to high yields. Tolerated substituents include electron rich or poor (hetero)aromatic rings, cycloalkyl and short or long chain alkyl groups bearing a variety of functional groups such as CF<sub>2</sub>, alkene, carboxylic ester, as well as protected ketone and diol, amine, or alcohol that can facilitate the post-reduction derivatization to nitrogen- and oxygen-containing molecules of higher complexity (Table 2).

Regarding access to internal allenes, the alkyne substitution pattern had no observable impact on the outcome of the reaction. Internal alkynes with alkyl (**15–19** and **25–26**) or (hetero) aryl (**6–14** and **20–23**) substituents performed equally well. Moreover, *ortho* substituents on the aryl rings had no detrimental effect on the reaction efficiency and selectivity (**11** and **12**). Additionally, a propargylic silyl ether did not interfere with the reaction (**19**), and a glycosyl ester (**20**) resisted interchange of the alkoxy moiety with methoxide generated in the reaction medium. On the other hand, the substitution mode at the carbon center adjacent to the carbonate leaving group had a notable impact on the profile of the reaction. While tertiary (**6–20**) as well as secondary (**21–23** and **26**) propargyl carbonates featuring alkyl groups delivered the desired allenes with satisfactory yields,  $\alpha$ -aryl propargylic carbonates proved to be less suitable substrates for the transformation. Hence, 1,3-bisarylallenes (e.g., **24**) were not accessible by this method, only providing degradation products. Accordingly, monoaryl 1,3-disubstituted allenes were only provided in moderate yields starting from  $\alpha$ -aryl propargylic carbonates. However, these monoaryl allenic compounds may still be afforded in good yields by simply inverting the substitution pattern of the propargyl substrate (e.g. **25**, path a vs. path b).

Regarding access to terminal allenes (**27–29**), these were delivered in satisfactory yields from primary propargyl carbonates, although alkynyl derivatives were also formed as minor regioisomeric products.<sup>11</sup> Alternatively, terminal allenes can be obtained from terminal propargylic carbonates, as illustrated by the reduction of the mestranol carbonate derivative (**30**). The generality of the method was further showcased by the successful reduction of enyne carbonates under our catalytic conditions, thus opening a new synthetic entry to valuable

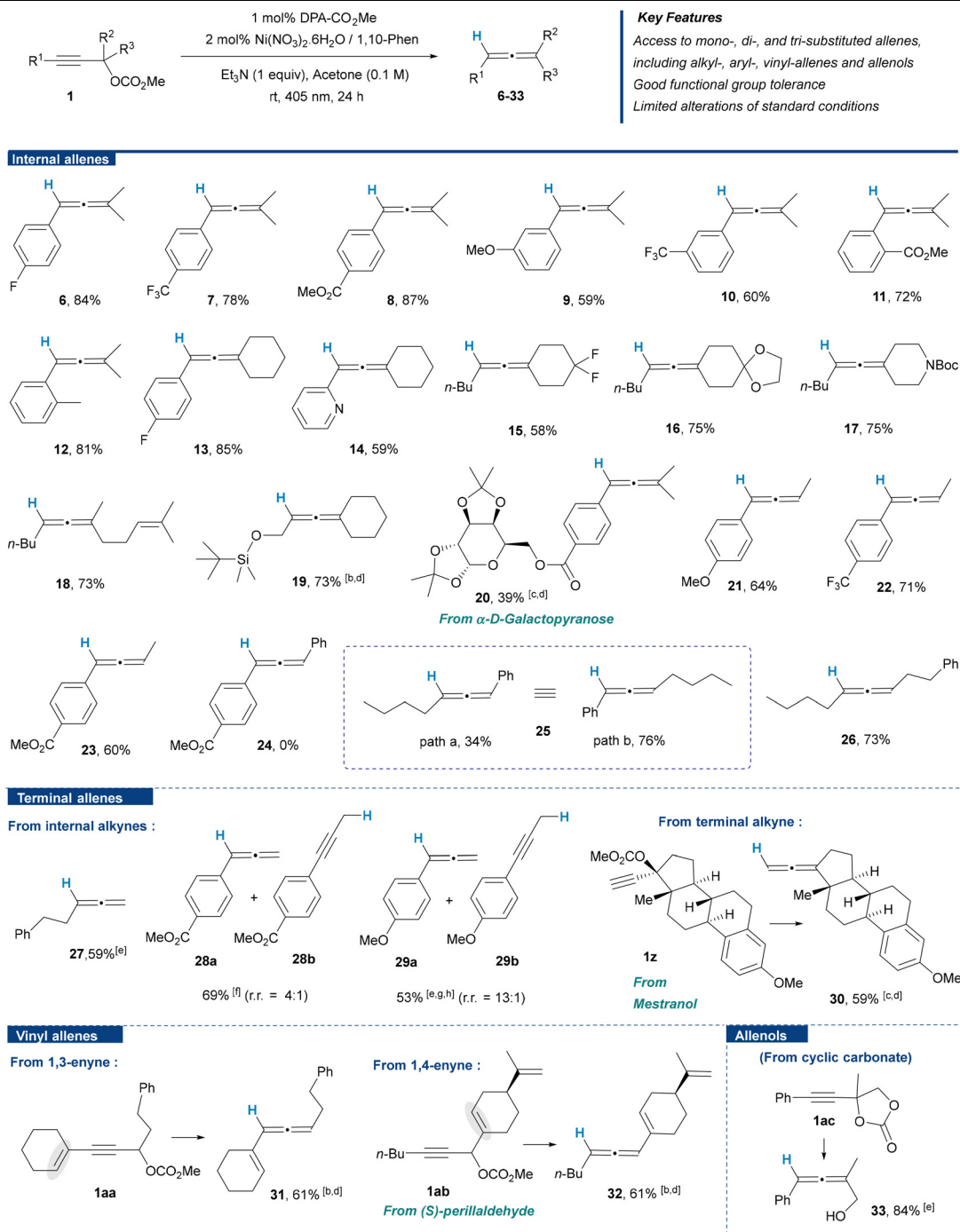
vinylallenes (**31**, **32**). Notably, electrophiles that are both allylic and propargylic offer several potential sites for the reduction to take place and therefore raise additional selectivity issues, *i.e.* competition between the allylic and propargylic functionalities. Remarkably, the 1,4-enyne substrate delivered the desired vinyl allene (**32**) chemoselectively as the sole reaction product. Finally, cyclic carbonates have also been shown to be competent electrophiles which further expand the diversity of accessible structures to include unprotected allenol derivatives, which have become ubiquitous as building blocks for downstream methodologies (**33**).<sup>12</sup> Importantly, in addition to proceeding in a sustainable fashion under very mild reaction conditions, the reduction process was easily amenable to simple scale up. For instance, a gram-scale synthesis of allene **6** could be achieved in high yield without the need for reoptimizing reaction parameters (Scheme 1).

### Mechanistic investigations

We then turned our attention to studying the pathway of this hydride-free Ni/photoredox reduction process and the exact role of Et<sub>3</sub>N (Fig. 2). We envisioned that the delivery of the hydrogen atom would proceed through the following pathway (Fig. 2A): (i) photooxidation of Et<sub>3</sub>N by the excited DPA\* ( $E^* = +1.19$  V vs. SCE in DMSO); (ii) deprotonation of the  $\alpha$ -amino C–H ( $pK_a = 14.7$  in MeCN) of the triethylamine radical cation species by methanolate, which is formed upon spontaneous decarboxylation of the Ni–OCO<sub>2</sub>Me intermediate,<sup>13</sup> and finally, (iii) protonation of the Ni–allenyl bond by the generated methanol to form the desired allene product. This was confirmed by a deuterium labelling experiment using fully deuterated triethylamine (Et<sub>3</sub>N-d<sub>15</sub>), which led to 90% deuterium incorporation into the nonexchangeable allenyl position. Interestingly, when the reaction was carried out in the presence of deuterated methanol, the desired product was obtained with a deuteration yield of 68%. This experiment indicates that methanol can serve as a protonolysis shuttle agent. The lower deuterium incorporation ratio is likely due to the presence of *in situ* generated CH<sub>3</sub>OH through deprotonation of the Et<sub>3</sub>N radical cation species by methanolate. Interestingly, when *i*Pr<sub>2</sub>NMe was used, we could detect the formation of hemiaminal ether species **34**, most likely ensuing from the capture of an iminium intermediate by methanolate (Fig. 2B). We speculated that the resulting *N*- $\alpha$ -carbon radical intermediate may undergo spontaneous single electron oxidation to provide this iminium intermediate.

Next, we aimed to evaluate whether propargyl/allenyl radical intermediates may be formed under photoredox conditions (Fig. 2C). As anticipated from a pathway involving radical species, the reaction was inhibited in the presence of 1 equivalent of 2,2,6,6-tetramethylpiperidinyloxy (TEMPO).<sup>14</sup> In addition, we observed a loss of stereochemistry when exposing enantiopure (*S*)-**1r** to catalytic conditions. The racemization process may involve either propargyl/allenyl radicals<sup>6b</sup> or metallotropic rearrangements of the oxidative addition nickel complex, possibly *via*  $\eta^3$ -propargyl/allenyl nickel intermediates.<sup>15</sup> Noteworthy, post-reduction photochemical erosion of



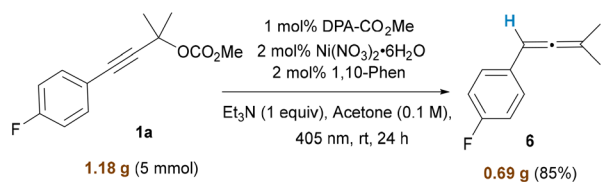
Table 2 Photochemical synthesis of allenes<sup>a</sup>

<sup>a</sup> Reactions performed on a 0.4 mmol scale unless otherwise stated. Isolated yields are given. <sup>b</sup> 0.2 mmol scale. <sup>c</sup> 0.1 mmol scale. <sup>d</sup> 5 mol% Ni/L, 2.5 mol% PC. <sup>e</sup> 3 mol% Ni/L, 1.5 mol% PC. <sup>f</sup> Yield refers to a mixture of inseparable regioisomers. <sup>g</sup> Yield of pure allene. <sup>h</sup> 72 h.

allene chirality may also proceed (see the ESI†).<sup>16</sup> Finally, the reaction of the cyclopropyl derivative **1ad** resulted in the formation of the non-opened cyclopropyl allene **35** as a major product, alongside minor byproducts that could not be isolated or identified. This result argues against the formation of the free allenyl radical intermediate as a main pathway. All

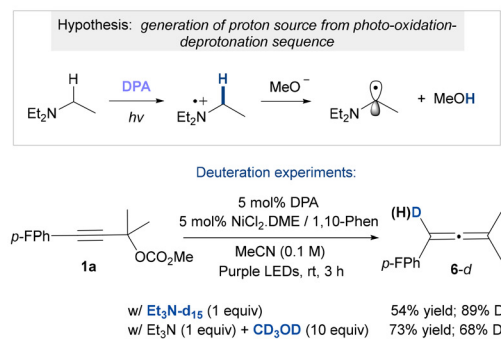
these experiments support the direct protonolysis of the oxidative addition allenyl-Ni complex involving a proton transfer process from the amine to the allene product. The detection of the hemiaminal ether **34** indicates that the trialkylamine reagent is converted into iminium species, most likely through a SET process from the α-aminoalkyl radical.



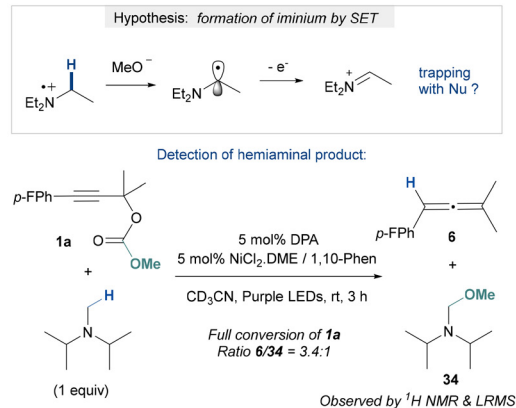


Scheme 1 Gram-scale synthesis.

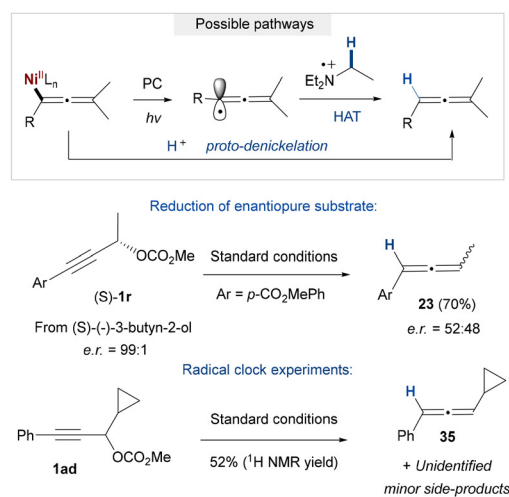
## A. Source of hydrogen atom



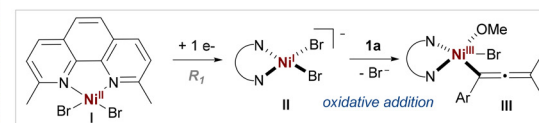
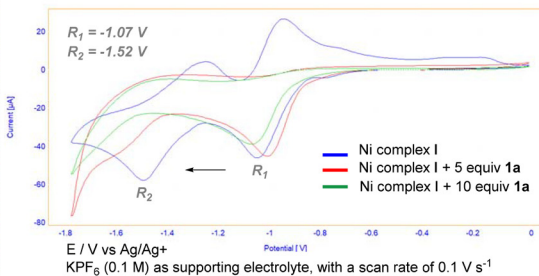
## B. Trialkylamine reaction outcome



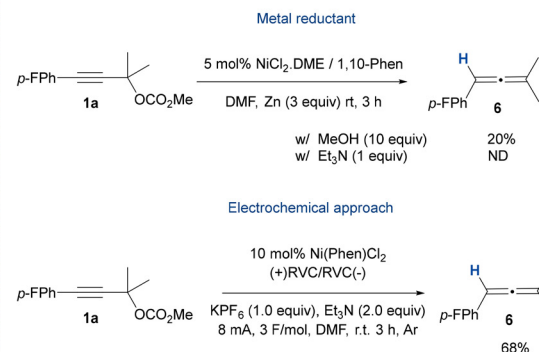
## C. Evaluation for Radical intermediates



## D. Cyclic voltammetry studies



## E. Comparison with Zn reductant and electroreduction



## F. Proposed mechanism

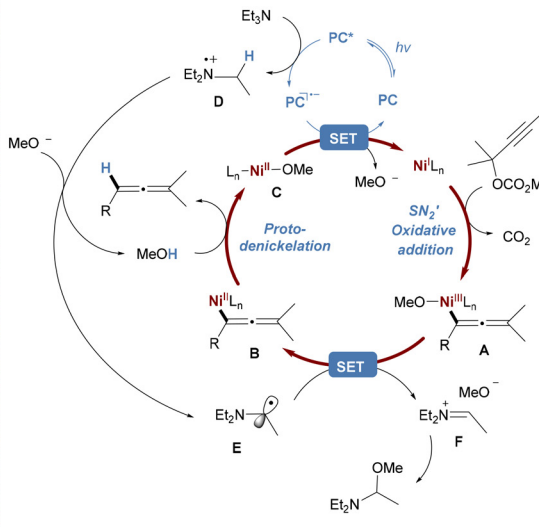


Fig. 2 Mechanistic experiments and comparison with alternative reductive methodologies.



Indeed, the CV of complex **I** exhibited two reversible reduction waves at  $-1.07$  V and  $-1.52$  V (*vs.* Ag/AgNO<sub>3</sub>) associated with Ni(II)/Ni(I) and Ni(I)/Ni(0) reductions (Fig. 2D). Upon the addition of several equivalents of propargyl carbonate **1a** (5 and 10 equiv.), an increase in current is observed at the first reduction peak associated with Ni(II)/Ni(I) reduction along with a complete loss of reversibility. A slight shift of the reduction peak is also observed, most likely due to pre-coordination of the substrate to nickel (Fig. S20, ESI†). This experiment is consistent with a facile oxidative addition of the propargyl carbonate to the electrogenerated Ni(I) species (**II**) to give a Ni(III)-allenyl species (**III**). Furthermore, a new reduction peak is observed at lower potential ( $-1.6$  V). We speculate that it may be associated with the reduction of a Ni(II)-allenyl intermediate presumably formed by rapid reduction of the Ni(III) transient species.

With this information in mind, we were interested in evaluating the effect of the reduction strategy on the catalytic efficiency (Fig. 2E). Notably, the use of zinc as a reductant, instead of the DPA/Et<sub>3</sub>N system under photoredox conditions, resulted in very low conversion to allene, thus indicating the significant influence of the photoredox promoted electron transfer process using homogeneous reductants.<sup>19</sup> We reasoned that electrochemical reduction may also stand as a reliable technology to promote the electron transfer in a controlled and smooth manner. Remarkably, the reaction also proceeded well under electrochemical conditions.<sup>20</sup> The desired allene could be obtained in good yield using RVC electrodes in an undivided cell under 8 mA constant current electrolysis. Satisfactorily, the use of Et<sub>3</sub>N, playing the roles of both a hydrogen source and a reductant also affords the possibility of avoiding the use of a sacrificial anode.<sup>21</sup>

Based on these investigations, a plausible mechanism for this nickel catalyzed, selective and hydride-free reduction of propargyl carbonates into allenes can be proposed, as shown in Fig. 2F. The pathway involves oxidative addition of the propargyl carbonate to low valent ligated Ni(I) species, which are generated *via* photocatalytic (or electro-) reduction, to give a Ni(III)-allenyl intermediate **A**, after spontaneous decarboxylation of the carbonate substituent. In parallel, photo- (or electro-) oxidation of the trialkylamine would generate the radical cation intermediate **D** that may undergo rapid deprotonation by the *in situ* generated methanolate anion. The resulting *N*- $\alpha$ -carbon radical intermediate **E** can participate in single electron transfer with the Ni(III)-allenyl intermediate **A** to give an iminium species **F** and the Ni(II)-allenyl intermediate **B**. A final protonolysis step with *in situ* generated methanol will deliver the desired allene product, and the Ni(II) species **C** can be reduced to regenerate the Ni(I) species.

## Conclusions

In conclusion, our study presents a new strategy for the synthesis of allenes through the development of a photocatalytic hydride-free protocol for the regioselective reduction of propar-

gyl carbonates. This method offers several key advantages, including the utilization of low loadings of inexpensive catalysts and ligands, alongside a sustainable and non-toxic solvent, acetone. Furthermore, our investigation unravels a novel mechanistic pathway involving hitherto undocumented protodenickelation of allenylnickel species,<sup>22</sup> shedding light on new avenues for catalytic hydrogen transfer processes. The use of trialkylamine as an inexpensive reductant and a source of hydrogen atoms further underscores the versatility and efficiency of our approach.

## Conflicts of interest

There are no conflicts to declare.

## Acknowledgements

This work was supported by the CNRS, the French Ministry of Research, the ICBMS, and the Université Claude Bernard Lyon 1. The NMR and Mass Centers of the Université Claude Bernard Lyon 1 are gratefully acknowledged for their contribution. T. H. thanks the Chinese Council Scholarship for a doctoral fellowship. A. A. thanks the Institut Universitaire de France (IUF) for its support. We thank Maurice Médebielle and Jérémy Merad for their help with cyclic voltammetry experiments and HPLC determination of enantiomeric ratios, respectively.

## Notes and references

- For representative books and reviews on allene chemistry, see: (a) *Modern Allene Chemistry*, ed. N. Krause and A. S. K. Hashmi, Wiley-VCH, Weinheim, 2004; (b) S. Ma, *Chem. Rev.*, 2005, **105**, 2829–2871; (c) A. Hoffmann-Röder and N. Krause, *Angew. Chem., Int. Ed.*, 2004, **43**, 1196–1216; (d) P. Rivera-Fuentes and F. Diederich, *Angew. Chem., Int. Ed.*, 2012, **51**, 2818–2828.
- Representative reviews: (a) S. Yu and S. Ma, *Chem. Commun.*, 2011, **47**, 5384–5418; (b) C. Q. O’Broin and P. J. Guiry, *J. Org. Chem.*, 2020, **85**, 10321–10333; (c) S. Du, A.-X. Zhou, R. Yang, X.-R. Song and Q. Xiao, *Org. Chem. Front.*, 2021, **8**, 6760–6782.
- (a) For an overview of early discoveries: J. Tsuji and T. Mandai, *Synthesis*, 1996, 1–24 Selected papers: (b) Y. Colas, B. Cazes and J. Gore, *Tetrahedron Lett.*, 1984, **25**, 845–848; (c) J. Tsuji, T. Sugiura, M. Yuhara and I. Minami, *J. Chem. Soc., Chem. Commun.*, 1986, 922–924; (d) T. Mandai, T. Matsumoto, Y. Tsujiguchi, S. Matsuoka and J. Tsuji, *J. Organomet. Chem.*, 1994, **473**, 343–352; (e) H. Ohmiya, M. Yang, Y. Yamauchi, Y. Ohtsuka and M. Sawamura, *Org. Lett.*, 2010, **12**, 1796–1799; (f) Y. Zheng, B. Miao, A. Qin, J. Xiao, Q. Liu, G. Li, L. Zhang, F. Zhang, Y. Guo and S. Ma, *Chin. J. Chem.*, 2019, **37**, 1003–1008.



- 4 (a) C. Deutsch, B. H. Lipshutz and N. Krause, *Angew. Chem., Int. Ed.*, 2007, **46**, 1650–1653; (b) C. Zhong, Y. Sasaki, H. Ito and M. Sawamura, *Chem. Commun.*, 2009, 5850–5852; (c) C. Deutsch, B. H. Lipshutz and N. Krause, *Org. Lett.*, 2009, **11**, 5010–5012; (d) H. Reeker, P.-O. Norrby and N. Krause, *Organometallics*, 2012, **31**, 8024–8030; (e) Y. Kim, H. Lee, S. Park and Y. Lee, *Org. Lett.*, 2018, **20**, 5478–5481 See also: (f) K. Guo and A. W. Kleij, *Angew. Chem., Int. Ed.*, 2021, **60**, 4901–4906.
- 5 (a) G. Durin, M.-Y. Lee, M. A. Pogany, T. Weyhermüller, N. Kaeffer and W. Leitner, *J. Am. Chem. Soc.*, 2023, **145**, 17103–17111; (b) F. Arcudi, L. Đorđević, N. Schweitzer, S. I. Stupp and E. A. Weiss, *Nat. Chem.*, 2022, **14**, 1007–1012; (c) C. Casadevall, D. Pascual, J. Aragon, A. Call, A. Casitas, I. Casademont-Reig and J. Lloret-Fillol, *Chem. Sci.*, 2022, **13**, 4270–4282; (d) T. Hu, M. Jaber, G. Tran, D. Bouyssi, N. Monteiro and A. Amgoune, *Chem. – Eur. J.*, 2023, e202301636.
- 6 Nickel-catalyzed reactions of propargyl electrophiles have been documented to provide effective ways of accessing allenic compounds. However, to the best of our knowledge, Ni-catalyzed reduction protocols remain unexplored to this date. For a review, see: (a) X. Liu, C. Jiao, S. Cui, Q. Liu, X. Zhang and G. Zhang, *ChemCatChem*, 2023, DOI: [10.1002/cctc.202300601](https://doi.org/10.1002/cctc.202300601) For selected nickel-catalyzed approaches towards allene synthesis from propargyl electrophiles, see: (b) R. Soler-Yanes, I. Arribas-Alvarez, M. Guisan-Ceinos, E. Bunuel and D. J. Cardenas, *Chem. – Eur. J.*, 2017, **23**, 1584–1590; (c) Y. Jin, H. Wen, F. Yang, D. Ding and C. Wang, *ACS Catal.*, 2021, **11**, 13355–13362; (d) Z.-Z. Zhou, X.-R. Song, S. Du, K.-J. Xia, W.-F. Tian, Q. Xiao and Y.-M. Liang, *Chem. Commun.*, 2021, **57**, 9390–9393.
- 7 J. W. Beatty and C. R. J. Stephenson, *Acc. Chem. Res.*, 2015, **48**, 1474–1484.
- 8 For recent examples of metallaphotoredox transformations involving tertiary amines as proton transfer reagents, see: Z.-Y. Gu, W.-D. Li, Y.-L. Li, K. Cui and J.-B. Xia, *Angew. Chem., Int. Ed.*, 2023, e202213281 See also ref. 5d.
- 9 For physical properties and previous (rare) uses of DPA as a photocatalyst, see: (a) Y. Chen, X. Wang, X. He, Q. An and Z. Zuo, *J. Am. Chem. Soc.*, 2021, **143**, 4896–4902; (b) M. Neumeier, U. Chakraborty, D. Schaarschmidt, V. de la Pena O'Shea, R. Perez-Ruiz and A. Jacobi von Wangelin, *Angew. Chem., Int. Ed.*, 2020, **59**, 13473–13478; (c) K. Xu, J. Zhao, X. Cui and J. Ma, *J. Phys. Chem. A*, 2015, **119**, 468–481; (d) V. Gray, D. Dzebo, A. Lundin, J. Alborzpour, M. Abrahamsson, B. Albinsson and K. Moth-Poulsen, *J. Mater. Chem. C*, 2015, **3**, 11111–11121; (e) S. K. Chattopadhyay, C. V. Kumar and P. K. V. Das, *Chem. Phys. Lett.*, 1983, **98**, 250–254.
- 10 An additional advantage of incorporating a functional group into the diphenylanthracene structure lies in the large increase in polarity facilitating separation of these photocatalysts from aliphatic allenes featuring polarities similar to that of DPA.
- 11 Primary propargylic carbonates have been shown to generate mixtures of terminal allenes and propargylic reduced compounds due to steric reasons: T. Mandai, T. Matsumoto, Y. Tsujiguchi, S. Matsuoka and J. Tsuji, *J. Organomet. Chem.*, 1994, **473**, 343–352.
- 12 J. M. Alonso and P. Almendros, *Chem. Rev.*, 2021, **121**, 4193–4252.
- 13 For a seminal paper on transition metal-catalyzed decarboxylative reactions of propargyl electrophiles, see: J. Tsuji, H. Watanabe, I. Minami and I. Shimizu, *J. Am. Chem. Soc.*, 1985, **107**, 2196–2198 For recent applications, see ref. 2b.
- 14 See the ESI† for details.
- 15 Similarly to related Pd-catalyzed processes, racemization may occur through interconversion of  $\eta^1$ -allenyl,  $\eta^1$ -propargyl and  $\eta^3$ -allenyl/propargyl ligands on the metal: (a) K. Mikami and A. Yoshida, *Angew. Chem., Int. Ed. Engl.*, 1997, **36**, 858–860; (b) H. Wang, H. Luo, Z.-M. Zhang, W.-F. Zheng, Y. Yin, H. Qian, J. Zhang and S. Ma, *J. Am. Chem. Soc.*, 2020, **142**, 9763–9771 The racemization of an optically active  $\eta^1$ -allenyl–palladium(II) species has been reported to occur via an  $\eta^3$ -allenyl/propargyl dimetallic complex: (c) S. Ogoshi, T. Nishida, T. Shinagawa and H. Kurosawa, *J. Am. Chem. Soc.*, 2001, **123**, 7164–7165.
- 16 For photosensitized racemization of allenes, see: O. Rodriguez and H. Morrison, *J. Chem. Soc. D*, 1971, 679.
- 17 T. Kerackian, D. Bouyssi, G. Pilet, M. Médebille, N. Monteiro, J. C. Vantourout and A. Amgoune, *ACS Catal.*, 2022, **12**, 12315–12325.
- 18 This ligand minimizes speciation issues with Ni(II) and undesired disproportionation reactions with Ni(I): T. Tang, A. Hazra, D. S. Min, W. L. Williams, E. Jones, A. G. Doyle and M. S. Sigman, *J. Am. Chem. Soc.*, 2023, **145**, 8689–8699.
- 19 The poor yield obtained with the Zn reductant may be attributed to the harsher electron transfer with a heterogeneous metal reductant and/or to undesired pathways involving organometallic intermediates.
- 20 For previous metal-catalyzed electroreductive cleavages of propargyl compounds, see: (a) S. Olivero and E. Duñach, *Tetrahedron Lett.*, 1997, **38**, 6193–6196; (b) H. Tanaka, H. Takeuchi, Q. Ren and S. Torii, *Electroanalysis*, 1996, **8**, 769–772.
- 21 For other recent examples of electrochemical strategies using Et<sub>3</sub>N as a sacrificial reductant, see Ni-catalyzed processes: (a) H. Li, C. P. Breen, H. Seo, T. F. Jamison, Y.-Q. Fang and M. M. Bio, *Org. Lett.*, 2018, **20**, 1338; (b) R. J. Perkins, A. J. Hughes, D. J. Weix and E. C. Hansen, *Org. Process Res. Dev.*, 2019, **23**, 1746–1751; (c) A. Claraz and G. Masson, *ACS Org. Inorg. Au*, 2022, **2**, 126–147, (Review) For specific examples of reduction processes, see: (d) B. Huang, L. Guo and W. Xia, *Green Chem.*, 2021, **23**, 2095–2103; (e) J. Ke, H. Wang, L. Zhou, C. Mou, J. Zhang, L. Pan and Y. R. Chi, *Chem. – Eur. J.*, 2019, **25**, 6911–6914.
- 22 For a recent mechanistic investigation of protodenickelation of Ni(II)-aryl species, see: P. E. Piszal, B. J. Orzolek, A. K. Olszewski, M. E. Rotella, A. M. Spiewak, M. C. Kozłowski and D. J. Weix, *J. Am. Chem. Soc.*, 2023, **145**, 8517–8528.

